

# The Influence of Isothermal Annealing and Structural Defects on Properties of Amorphous $\text{Fe}_{78}\text{Si}_{11}\text{B}_{11}$ with High Magnetization Saturation

KATARZYNA BLOCH\*

Institute of Physics, Faculty of Production Engineering and Materials Technology, Czestochowa University of Technology,  
19 Armii Krajowej Str., 42-200 Czestochowa, Poland

*This paper presents the results of numerical analysis of the primary magnetization curves, which were obtained under the assumptions of the theory of approach to ferromagnetic saturation described in by H. Kronmüller. Test samples of the  $\text{Fe}_{78}\text{Si}_{11}\text{B}_{11}$  alloy were tape-shaped materials, which were subjected to isothermal annealing, not causing their crystallization. The investigated ribbons (tapes) were characterized by a very high saturation magnetization value of approximately 2T, which the thermal treatment has increased by about 10%. It was found that reason for the change of saturation magnetization of the investigated samples was the local rearrangement of atoms due to diffusion processes leading to the release of free volumes to the surface and combining of them into larger unstable defects called pseudodislocational dipoles.*

**Keywords:** magnetization saturation, free volumes, pseudodislocational dipoles, isothermal annealing

Since the beginning of the first metallic glass produced amorphous materials, these have become the object of interest of scientists from many fields of science but in particular specialists in physics and materials science. The group of precursors of amorphous materials include thin films produced by electrochemical method [1-3], which the application was not exactly satisfactory. The big breakthrough in the production of amorphous alloys came when Pond and Maddini [4] and Chen and Miller [5] presented to the world the first work in which the amorphous sample was a tape with a thickness of several tens of micrometers. Since then, a number of methods enabling the production of amorphous tapes to the critical thickness can now reach over several tens of micrometers [6, 7]. A particularly interesting group of amorphous alloys due to the unique ability of application have become FeCoB amorphous matrix materials exhibiting magnetically soft ferromagnetic properties [8, 9]. Initially, when GubaLow [10] and others obtained amorphous ferromagnetic, this fact was for them unacceptable. The reason for this was conviction existing at the time, that the ferromagnetic state was associated exclusively with crystalline materials, for which a well-described and known domain structure was present. As it turned out later, for the existence of ferromagnetism crystalline structure is not necessary. The amorphous tapes are typically made on a single rapidly rotating cylinder which is cooling the melt, giving access to cooling speeds within  $10^3 - 10^6 \text{K/s}$  [11, 12]. So huge cooling rates are the reason for the so-called freezing of the structure and limiting the diffusion of atoms over long distances, which blocks the nucleation. Generally in ferromagnetic amorphous materials there is constant search for new material that may be replacement for commercially produced and used FeSi based materials. Absence of crystalline structure and to some extent random distribution of atoms in a volume of these materials are a good reasons for their good properties and for describing the properties of the magnetically soft ferromagnetic alloys. For those ferromagnetics, we observe a low value of

coercive field, and what is directly related the small losses for remagnetization and magnetostriction. [13-15]. Some of the Fe-based alloys can exhibit the so-called magnetocaloric effect [16, 17]. They are characterized by the relatively high saturation magnetization and magnetic permeability [18]. The combination of these positive attributes of amorphous ferromagnetic materials may be the reason for a significant reduction of losses in electricity transmission, taking into account the positive impact on the environment. Reduction of transmission losses of energy in terms of even one of the city is a huge financial saving. Therefore, research on the properties of ferromagnetic amorphous magnetically soft materials is so important. Currently, we distinguished a large group of such alloys [19-21]. In addition, the aforementioned properties can be improved by thermal treatment. The heat treatment process must be designed and may involve heating the material to a suitable temperature in a predetermined time or at the annealing at a constant temperature and a specified time [22, 23]. Mostly the process of thermal interference to the amorphous sample leads to its nanocrystallization and then, if any, improvement of the magnetic properties is explained based on the random anisotropy model, which was proposed by Herzer [24, 25]. It also happens that the same heat treatment process without nanocrystallization of amorphous precursor leads to a homogeneous structure and a local increase in the number of magnetic moments in a given volume. It is known that in amorphous alloys there exists chemical and topological disorder, which is reflected by fluctuations in composition and density. It is relatively easy to explain the improvement of soft magnetic properties of nanocrystalline alloys in comparison to amorphous alloys where it is difficult to demonstrate the reasons for improving the properties within the amorphous state. Using the theory of approach to ferromagnetic saturation developed by H. Kronmüller and based on the theory of W. H. Brown's for model of micro-magnetism one can perform numerical analysis of the original

\* email: 23kasial@wp.pl

magnetization curves [26] and investigate in an indirect way the real structure of such alloys. In the amorphous alloys there are two types of structure defects that can be related to the defects described in crystal structure. The structure of amorphous and nanocrystalline materials may be subjected to computer simulation using Finite Element Method. The research presented in this paper may give rise to thermodynamic numerical analysis [27-30].

The paper presents study results for samples in the form of tapes subjected to the process of isothermal annealing, which has not led to their nanocrystallization and was the reason for the increase in saturation magnetization.

### Computational details

The test specimens were prepared from the ingredients are of high purity: Fe – 99.98% at., Si – 99.999% at. Boron was added to the preparation in the form of an alloy with the composition Fe<sub>54.6</sub>B<sub>45.6</sub>. Components weighed in a suitable ratio have been melted in an arc furnace under an atmosphere of argon. During the melting process additionally an oxygen absorbing titanium was used to prevent oxidation due to remainings of oxygen in the chamber. Melting alloy components performed with operating current of 380 A and an Ar 0.3 atmosphere. The prepared ingot weighing about 10 g were crumbled into smaller portions. They were then placed in a quartz capillary and using the method of melt spinning they were cast to tapes. Tapes were also cast under a protective atmosphere of argon at the linear speed of the copper roll 30 m/s. The product has thickness of about 35 microns and the width of 3 mm. Thus formed, the tapes were divided and a series of thermal treatments were done: 650 K/15min. After the heat treatment samples were examined using X-ray diffraction. Used to studies X-ray diffractometer (BRUKER D8 Advance) was equipped with a CuK $\alpha$  X-ray tube. The examination was performed in a 2 $\theta$  angle from 30° to 120° at a resolution of 0.02° and a measurement time of 5 s per step. Among the annealed tapes these in which crystalline phases were not detected were used. Measurement of magnetization as a function of magnetic field strength was carried out using a vibrating magnetometer Lakeshore 7300 working to the value of magnetic field 2 T. Measurement error according to data from the manufacturer is 0.001 A/m. The initial magnetization curves and static magnetic hysteresis loops were measured.

Using the initial magnetization curves their analysis has been made in accordance with the assumptions of the theory of H. Kronmuller [1, 2].

### Theoretical introduction

According to H. Kronmuller [31] magnetization in strong magnetic field above anisotropy field  $\left(H > \frac{2K_{eff}}{\mu_0 M_s}\right)$  can be written as:

$$\Delta M = \Delta M_{wew} + \Delta M_{para} + \Delta M_{def} \quad (1)$$

where:  $(\Delta M_{para})$  – results from damping of thermally excited spin waves by the external field,  $(\Delta M_{wew})$  – rises from internal fluctuations (like anisotropy and density change),  $(\Delta M_{def})$  – is related to the structural defects.

The first factor occurring in the equation (1) is so small (of order:  $\Delta M_{wew} \sim 10^{-6}$ ), that in comparison with the other can be omitted [1, 31]. Therefore, the magnetization in the vicinity of the so-called. Knees [33] describes the equation [34, 35]:

$$\mu_0 M(H) = \mu_0 M_s \left[ 1 - \frac{a_{1/2}}{(\mu_0 H)^{1/2}} - \frac{a_1}{(\mu_0 H)^1} - \frac{a_2}{(\mu_0 H)^2} \right] + b(\mu_0 H)^{1/2} \quad (2)$$

where:  $M_s$  – spontaneous magnetization,  $\mu_0$  – magnetic permeability of vacuum,  $H$  – the intensity of the magnetic field,  $a_i$  ( $i = 1/2, 1, 2$ ) – coefficients of the linear fit, which correspond to the free volume, and linear defects,  $b$  – the slope of the linear fit corresponds to the thermally induced damping of spin waves by a magnetic field of high intensity.

The terms appearing in equation (2) are described by 3, 4 and 5.

$$\frac{a_{1/2}}{(\mu_0 H)^{1/2}} = \mu_0 \frac{3}{20 A_{ex}} \left( \frac{1+r}{1-r} \right)^2 G^2 \lambda_s^2 (\Delta V)^2 N \left( \frac{2 A_{ex}}{\mu_0 M_s} \right)^{1/2} \frac{1}{(\mu_0 H)^{1/2}} \quad (3)$$

$$\frac{a_1}{\mu_0 H} = 1, 1 \mu_0 \frac{G^2 \lambda_s^2}{(1-\nu)^2} \frac{N b_{eff}}{M_s A_{ex}} D_{dp}^2 \frac{1}{\mu_0 H} \quad (4)$$

$$\frac{a_2}{\mu_0 H^2} = 0, 456 \mu_0 \frac{G^2 \lambda_s^2}{(1-\nu)^2} \frac{N b_{eff}}{M_s^2} D_{dp}^2 \frac{1}{(\mu_0 H)^2} \quad (5)$$

where:  $\Delta V$  – means a change in volume caused by the presence of point defects which are characterized by a bulk density  $N$ ,  $A_{ex}$  – exchange constant,  $G$  – shear modulus,  $\nu$  – Poisson's ratio,  $\lambda_s$  – magnetization constant.

Equation 3 describes the relationship for  $i = 1/2$  and relates to the interaction of point defects in the process of magnetization of the ferromagnetic known as approach to saturation area. While the equation 4 for  $i = 1$  ( $D_{dip} < l_H$ , where  $l_H$  – Exchange distance) and eq. 5 for  $i = 2$  ( $D_{dip} > l_H$ ) describes the effect of linear defects (pseudo-dislocational dipoles) on the course of the further process of magnetization in terms of the described area. The distance of exchange ( $l_H$ ) is then defined as the distance within which at least two dipole dislocations.

$$l_H = \sqrt{\frac{2 A_{ex}}{\mu_0 H M_s}} \quad (6)$$

where  $A_{ex}$  is the exchange distance, defined as:

$$A_{ex} = \frac{M_s D_{sp}}{2 g \mu_B} \quad (7)$$

where  $D_{sp}$  is a parameter of spin wave stiffness described by equation:

$$D_{sp} = \frac{k}{4\pi} \left( \frac{2, 612 \mu_B \mu_0}{M_0 c_{3/2}} \right)^{3/2} \quad (8)$$

where:  $M_0$  – means the magnetic polarizations in 5 K,  $C_{3/2}$  – staLa determined by fitting the temperature dependence of the magnetization of law as a function of magnetic field strength ( $\mu_0 H = 1$  T).

Term  $b(\mu_0 H)^{1/2}$  is related to the Holstein-Primakoff paraproces [36], describing the increase in the magnetization determined by the above relationship (5). The slow growth of the magnetization occurs as a result of thermal attenuation of spin waves [37]. The  $b$  expression can be determined using the relationship.

$$b = 3, 54 g \mu_0 \mu_B \left( \frac{1}{4\pi D_{sp}} \right)^{3/2} kT (g \mu_B)^{1/2} \quad (9)$$

where:  $k$  – Boltzman constant,  $\mu_B$  – Bohrs magneton,  $g$  – gyromagnetic factor.

If a strong magnetic field magnetization process is dominated by the presence of point defects one can then determine their bulk density using the relationship:

$$N_{\max} = \frac{3}{4\pi} \frac{1}{l^3 H} \quad (10)$$

Where the process of magnetization of ferromagnetic in approach to saturation area occurs under rotation of the magnetization vector in the vicinity of line defects (pseudodislocational dipoles) is satisfied, and the right 4 is fulfilled one can estimate the density of the surface according to:

$$N_{\text{dip}} = \frac{1}{l^2 H} \quad (11)$$

The use of this theory gives the opportunity to know the real structure of the alloy and its impact on the process of magnetization in the field known as approach to ferromagnetic saturation area.

## Results and discussions

Figure 1 shows the X-ray diffraction images of the samples in the form of a tape in a state after solidification and heat-treated at a 650 K temperature and for a soaking time 15min.

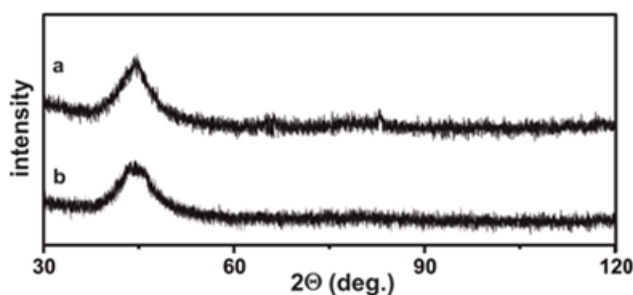


Fig. 1. X-ray patterns obtained for examined samples in the state after solidification (a) and after the isothermal heating process 650 K/15min (b)

The X-ray diffraction patterns for both the sample in a state after solidification and after heat treatment are similar and consist only of a broad peak, which is typical of amorphous materials. This effect is related to the dispersion of the reflected X-rays from a samples surface for which it is impossible to determine the appropriate pattern. In figure 2 static magnetic hysteresis loops are given measured for the examined samples in the state after solidification and after the isothermal heating process.

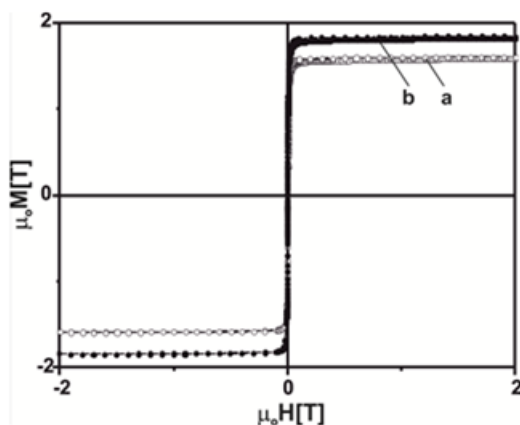


Fig. 2. Static magnetic hysteresis loops obtained for the examined samples in the state after solidification (a) and after the isothermal heating process 650 K/15min (b)

Shapes of static magnetic hysteresis loops for both examined samples are similar. In the central part of the M-H, value of the coercive force is small, indicating that the samples can be classified as soft magnetic materials. For the sample after solidification the value of the coercive force was 274 A/m and it was higher than for a sample after isothermal heating process ( $H_c = 237$  A/m). The reason things are taking place lies in the heating process where relaxation processes are occurring. The energy delivered to the samples volume is sufficient for atoms jumping while maintaining the amorphous state. This means that this energy only allows migration of groups of atoms through certain barriers appointing another metastable states.

Studied alloys demonstrate quite a high value of saturation magnetization, which equals 1.58 T and 1.82 T for alloy in the as-quenched state and after annealing, respectively. The observed changes in the magnetic properties are the result of the annealing process. During the heat treatment of investigated alloy there occurs a structural relaxation, which leads to a higher atomic packing density within the structure. This results in situation, where more atoms are taking locally ordered positions.

In figures 3 and 4 the curves of relative magnetization  $M/M_s$  versus induction of magnetizing field for the amorphous  $\text{Fe}_{78}\text{Si}_{11}\text{B}_{11}$  alloy, in the as-quenched state and after annealing, are shown.

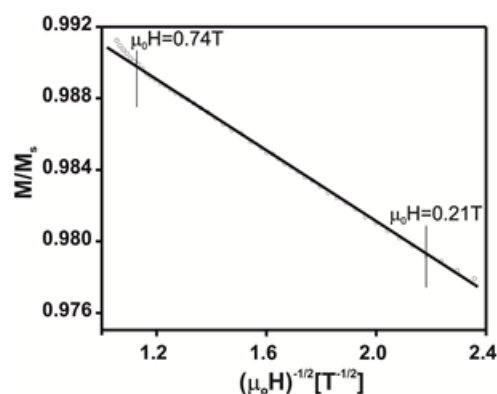


Fig. 3. Relative magnetization  $M/M_s$  versus induction of magnetizing field  $(\mu_0 H)^{-1/2}$  for the amorphous  $\text{Fe}_{78}\text{Si}_{11}\text{B}_{11}$  alloy, in the as-quenched state

In the magnetizing field induction range  $(\mu_0 H)^{-1/2}$  for the alloy in the as-quenched state is observed. (fig. 3). We may state that in this magnetic field range the magnetization process in this alloy is dominated by rotation of magnetic moments near point-like defects [33, 35, 38-40].

For the sample after annealing, in magnetic field induction range from 0.36 T to 0.11 T, the similar shapes of dependence of the reduced magnetization on  $((\mu_0 H)^{-1/2})$  have been observed (fig. 4a). It is also connected to the rotations of the magnetization vectors in the vicinity of the point defects. Additionally, in the case of  $\text{Fe}_{78}\text{Si}_{11}\text{B}_{11}$  alloy after annealing the linear dependence of  $M/M_s$  versus  $((\mu_0 H)^{-1})$  in magnetic field induction range from 0.11 T to 0.40 T is found (fig. 4b). Such behavior proves that in this magnetizing field range the magnetization process takes place by microscopic rotations of magnetic moments near quasi-dislocation dipoles for which the reciprocal of the exchange length ( $\kappa$ ) and dipole width ( $D_{\text{dip}}$ ) fulfills the rule  $\kappa D_{\text{dip}} < 1$  [32, 35, 38].

In stronger magnetic fields, of more than 0.74 T and 0.40 T for the samples in the as-quenched state and annealed state, respectively, a linear dependence  $\mu_0 M_s ((\mu_0 H)^{1/2})$  has been observed (fig. 5 a, b). It indicates



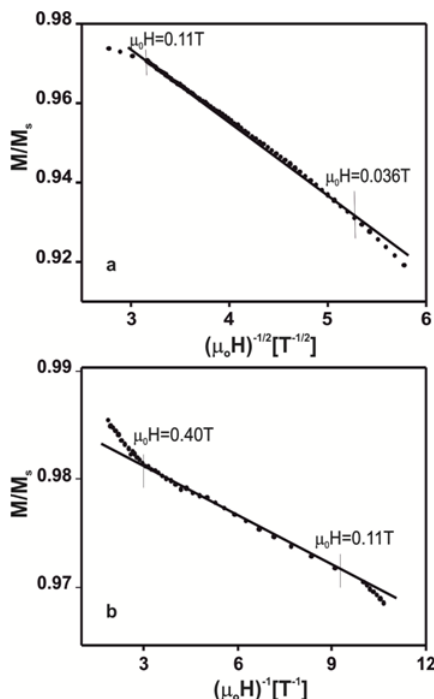


Fig. 4. Relative magnetization  $M/M_s$  versus induction of magnetizing field:  $(\mu_0 H)^{-1/2}$  (a) and  $(\mu_0 H)^{-1}$  (b) for the amorphous  $\text{Fe}_{78}\text{Si}_{11}\text{B}_{11}$  alloy, after annealing

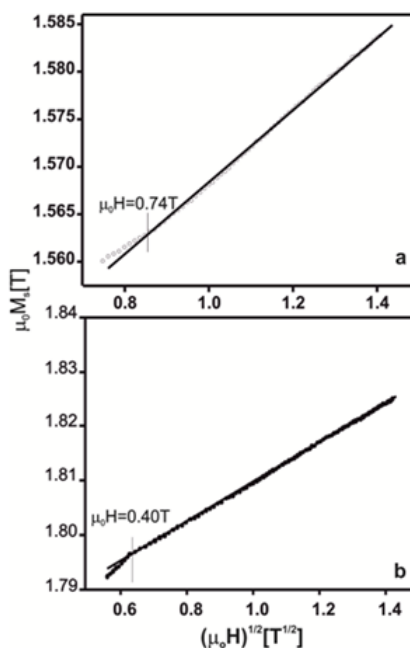


Fig. 5. The high-field magnetization curves  $\mu_0 M_s ((\mu_0 H)^{1/2})$  for the amorphous alloy sample in the state after solidification (a) and after the isothermal heating process 650 K/ 15min (b)

PARAMETERS	$a_{1/2} [\text{T}^{1/2}]$	$a_1 [\text{T}^{1/2}]$	$b [\text{T}^{1/2}]$	$D_{sp} [10^{-2} \text{eVnm}^2]$
<i>As-cast state</i>	0.0156	-----	0.039	58
<i>After thermal treatment</i>	0.0182	0.0016	0.037	60

**Table 1**  
DATA FROM HIGH-FIELD  
MAGNETIZATION  
CURVES

that in this field range the magnetization process is governed by the Holstein – Primakoff process [36, 39].

The results obtained from analysis of the high-field magnetization curves are presented in table 1.

Using the equation (9) the parameter  $D_{sp}$  was determined. This parameter is connected with the changes in the nearest neighborhood of the iron atoms. The value of ( $D_{sp}$ ) for the annealing sample of the investigated alloy is higher, which means that distances between the closest magnetic neighbors are smaller than in case of the alloy in the as-quenched state [22]. The higher value of spin wave stiffness parameter ( $D_{sp}$ ) for the annealing alloy value indicates a high concentration of magnetic atoms per unit volume, and confirms the high value of the saturation magnetization.

## Conclusions

On the basis of the performed investigations, it can be stated that the obtained alloy of  $\text{Fe}_{78}\text{Si}_{11}\text{B}_{11}$  in the as-quenched state and after annealing, was amorphous. Moreover, it was found that the heat treatment of alloy has an influence on the magnetic properties of these materials. During the heat treatment of the alloy occurs rearrangement of atoms, that leads to a reduction in the distance between magnetic atoms. This improves the chemical short-range order. From measurements of magnetization under the influence of strong magnetic fields, it was found that the magnetization process of investigated alloy was influenced by point and linear defects (called quasi-dislocational dipoles). In the as-quenched sample, the first law of the approach to ferromagnetic saturation has been fulfilled. In the case of annealing alloy, the magnetization process within strong magnetic fields was found to be influenced by both point

defects and quasi-dislocational dipoles. In higher magnetic fields the magnetization process for both samples is connected with the Holstein-Primakoff paraprocess. From analysis of the magnetization curves, the spin wave stiffness parameter for the investigated alloy was determined. The higher value of this parameter for annealing sample indicates a higher value of the atomic packing density of this alloy.

## References

- 1.H. KRONMULLER, M. FÄHNLE, Cambridge University Press 2003
- 2.N. LENG, H. KRONMÜLLER, Phys. Status Solidi B, 95, 1986, p. 621
- 3.A. BRENNER, D.E. COUCH, E.K. WILLIAMS, J. Res. Natl. Bur. Stand., 44, 1950, p. 109
- 4.R.B. POND JR., R. MADDIN, Transactions of the Metallurgical Society of the American Institute of Mechanical Engineers (SAUS), 245, 1969, p. 2475,
- 5.H.S. CHEN, C.E. MILLER, Review of Scientific Instruments, 41, 1970, p. 1237.
- 6.A. INOE, F. L. KONG, S. L. ZHU, E. SHALAN, F. M. AL-MARZOUKI, Intermetallics, 58, 2015, p. 20.
- 7.M. NABIALEK, P. PIETRUSIEWICZ, K. BLOCH, Journal of Alloys and Compounds, 628, 2015, p. 424.
- 8.F. G. CHEN, Y. G. WANG, J. Alloys Comp., 584, 2014, p. 337-380
- 9.M. NABIALEK, P. PIETRUSIEWICZ, K. BLOCH, MICHAŁ SZOTA, Int. J. Mater. Res. (formerly Z. Metallkd.), 106, 2015, p. 1.7
- 10.A. I. GUBANOW, Fiz. Tverd. Tela., 2, 1960, p. 502.
- 11.P. DUWEZ, R. H. WILLENS, Trans. Met. Soc. AIME, Rapid Quenching of Liquid Alloys, Transactions of the Metallurgical Society of the American Institute of Mechanical Engineers (SAUS), 227, 1963, p. 362
- 12.P. PIETRUSIEWICZ, K. BLOCH, M. NABIALEK, S. WALTERS, Acta. Phys. Pol. A, 127, 2015, p. 397.
- 13.M. NABIALEK, J. Alloys Comp., 642, 2015, p. 98.
- 14.P. PIETRUSIEWICZ, M. NABIALEK, M. SZOTA, K. PERDUTA, Arch. Metall. Mater., 57, 2012, p. 255.

- 15.M. NABIALEK, M. DOSPIAL, M. SZOTA, P. PIETRUSIEWICZ, S. WALTERS, D. SKOWRON, *Mater. Sci. Eng. B-ADV*, 178, 2013, p. 99.
- 16.J. GONDRO, K. BLOCH, M. NABIALEK, S. WALTERS, *Acta. Phys. Pol. A*, 127, 2015, p. 606.
- 17.J. GONDRO, J. SWIERCZEK, K. BLOCH, J. ZBROSZCZYK, W. CIURZYNSKA, J. OLSZEWSKI, *Phys. Rev. B: Condens. Matter*, 445, 2014, p. 37.
- 18.K. BLOCH, *J. Magn. Magn. Mater.*, 390, 2015, p. 118.
- 19.K. M. GRUSZKA, M. NABIALEK, K. BLOCH, J. OLSZEWSKI, *Nukleonika*, 60, 2015, p. 23.
- 20.P. PIETRUSIEWICZ, M. NABIALEK, M. DOSPIAL, K. GRUSZKA, K. BLOCH, JOANNA GONDRO, P. BRAGIEL, M. SZOTA, Z. STRADOMSKI, *J. Alloys Comp.*, 615, 2014, p. S67.
- 21.X. D. FAN, H. MEN, A. B. MA, B. L. SHEN, *J. Magn. Magn. Mter.*, 325, 2013, p. 22.
- 22.K. BLOCH, M. NABIALEK, *Acta. Phys. Pol. A*, 127, 2015, p. 442.
- 23.K. BLOCH, M. NABIALEK, P. PIETRUSIEWICZ, J. GONDRO, M. DOSPIAL, M. SZOTA, K. GRUSZKA, *Acta. Phys. Pol. A*, 126, 2014, p. 108.
- 24.G. HERZER, *IEEE Trans. Magn.*, 25, 1989, p. 3327.
- 25.G. HERZER, *IEEE Trans. Magn.*, 26, 1990, p. 1397.
- 26.W.F. BROWN, *Physical Review*, 58, 1940, p. 736.
- 27.L.A. DOBRZANSKI, A. SLIWA, W. SITEK, *Surf. Eng. 5 ISEC*, 2006, p. 26.
- 28.A.SLIWA, B. BONEK, J. MIKULA, *App. Sur. Sci.*, 388, 2016, p. 174.
- 29.L.W. UKOWSKA, A. SLIWA, J. MIKULA, M. BONEK, W. KWASNY, M. SROKA, D. PAKULA, *Arch. Metall. Mater.*, 61, 2016, p. 149.
- 30.A.SLIWA, J. MIKULA, K. GOLOMBEK, T. TANSKI, B. BONEK, W. KWASNY, Z.BRYTAN, *App. Sur. Sci.*, 388, 2016, p. 281.
- 31.H. KRONMÜLLER, *J. Appl. Phys.*, 52, 1981, p. 1859.
- 32.H. KRONMÜLLER, M. FÄHNLE, M. DOMANN, H. GRIMM, R. GRIMM, B. GROGER, *J. Magn. Magn. Mater.*, 13, 1979, p. 53.
- 33.F. BLAISFORD, *Magnetic Materials*, PWN, 1964.
- 34.H. KRONMÜLLER, *IEEE Trans. Magn. MAG-15*, 1979, p. 1218.
- 35.M. VAZQUEZ, W. FERNENGEL, H. KRONMÜLLER, *Phys. Status Solidi A*, 115, 1989, p. 547.
- 36.T. HOLSTEIN, H. PRIMAKOFF, *Phys. Rev.*, 59, 1941, p. 388.
- 37.O. KOHMOTO, *J. Appl. Phys.* 53, 1982, p. 7486.
- 38.M. NABIALEK, P. PIETRUSIEWICZ, M. DOSPIAL, M. SZOTA, K. BLOCH, K. GRUSZKA, K. OGA, S. GARUS, *J. Alloys Comp.*, 615, 2014, p. S51.
- 39.K. SOBCZYK, J. ZBROSZCZYK, M. NABIALEK, J. OLSZEWSKI, P. BRĄGIEL, J. SWIERCZEK, W. CIURZYNSKA, A. LUKIEWSKA, M. LUBAS, M. SZOTA, *Arch. Metall. Mater.*, 53, 2008, p. 855.
- 40.NABIALEK, M., PIETRUSIEWICZ, P., SZOTA, M., ABDULLAH, M.M.A.B., SANDU, A.V., *Rev. Chim. (Bucharest)*, **68**, no. 1, 2017, p. 22.

Manuscript received: 14.12.2016